Article

In Situ Application of Berberine-Loaded Liposomes on the Treatment of Osteomyelitis

Siting Wang, Tianlong Zhao, Yuping Sun, Sipan Li, Danya Lu, Mengmeng Qiu, Baofei Yan,
Jingwen Yang, Zhitao Shao, Yuqi Yin, Shaoguang Li,* and Tingming Fu*

ACCESS | 📊 Metrics & More | 📖 Article Recommendations | 🆂🅸 Supporting Information

ABSTRACT: Osteomyelitis is a major challenge in global healthcare, as it requires the simultaneous management of bone defects and bacterial infections, which poses considerable difficulties for orthopedic clinicians. In this study, we developed berberine liposome-modified bone cement specifically aimed at treating osteomyelitis induced by *Staphylococcus aureus*. We characterized the physical properties of this modified bone cement, conducted in vitro antibacterial assays to evaluate its efficacy in eradicating *Staphylococcus aureus* biofilm, established an in vivo rat model of osteomyelitis, and performed histopathological assessments alongside micro-CT analysis of bone parameters. The results indicated that the berberine liposome-modified bone cement exhibited favorable biodegradability and sustained-release characteristics, with a drug release rate of more than 90% within 14 days, while effectively eliminating bacterial biofilm with a biofilm eradication rate of up to 80% and facilitating bone repair with a bone volume fraction of 80%. This innovative treatment demonstrated both safety and efficacy in addressing tibial osteomyelitis in rats, thereby offering novel insights and methodologies for clinical interventions against osteomyelitis.
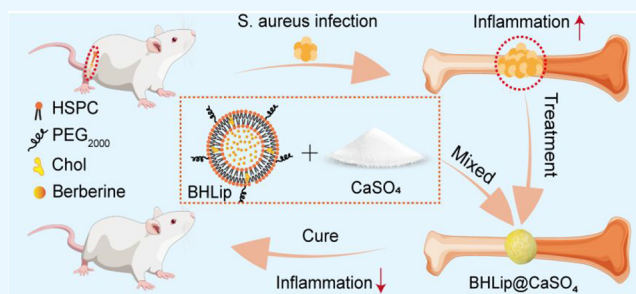
1. INTRODUCTION

Osteomyelitis is an inflammatory disease caused by purulent bacterial infection of the bone marrow, bone cortex, and periosteum. While most cases of osteomyelitis arise from hematogenous spread, it can also result from infections following trauma or surgical procedures.[1,2] Osteomyelitis afflicts millions of patients globally each year, presenting an enduring challenge for orthopedic professionals worldwide and imposing substantial burdens on both patients and society.[3]

Bacterial infections are the main causative agents of osteomyelitis, with *Staphylococcus aureus* being the most prevalent single pathogen.[4] An important and well-studied mechanism of *S. aureus* pathogenesis in osteomyelitis is the formation of biofilm,[5,6] which limits the diffusion of antibiotics and inhibits immune cell penetration.[7] Establishing local and systemic infection control is a key principle in the treatment of osteomyelitis, most patients with osteomyelitis require surgical debridement and systemic antibiotic therapy.[8] However, prolonged antibiotic therapy (oral or intravenous administration) affects normal tissues and causes various side effects.[9] Antibiotic bone cement can directly target the infection site and deliver high doses of antibiotics, thereby minimizing the side effects associated with systemic antibiotic therapy.[10] Nevertheless, the conventional approach to preparing antibiotic bone cement involves simply adding antibiotics to the bone repair material, which limits therapeutic efficacy due to

the difficulty of free antibiotics penetrating biofilms. Therefore, there is an urgent need for innovative methods for preparing antibiotic bone cement in clinical settings.[11]

Liposomes are the most widely used biocompatible and biodegradable nanodelivery system that can efficiently treat bacterial infections[12] since they can penetrate biological membranes and fuse with the bacterial outer membrane, releasing drugs directly into the cells for optimal efficacy.[13,14] Cholesterol microdomains in the lipid membrane of highly cholesterol-engineered liposomes have been reported to bind hemolysins and release drugs through pores stimulated by membrane-damaging toxins, thereby effectively killing bacteria.[15] Recently, we developed a liposome enriched with cholesterol and encapsulated with berberine. Our findings revealed that this berberine-loaded liposome significantly inhibited the growth of *S. aureus* and effectively disrupted biofilm formation.[16] Berberine is a quaternary benzylisoquinoline alkaloid derived from the traditional Chinese medicine Huanglian[17] and possesses antibacterial, anti-inflammatory,
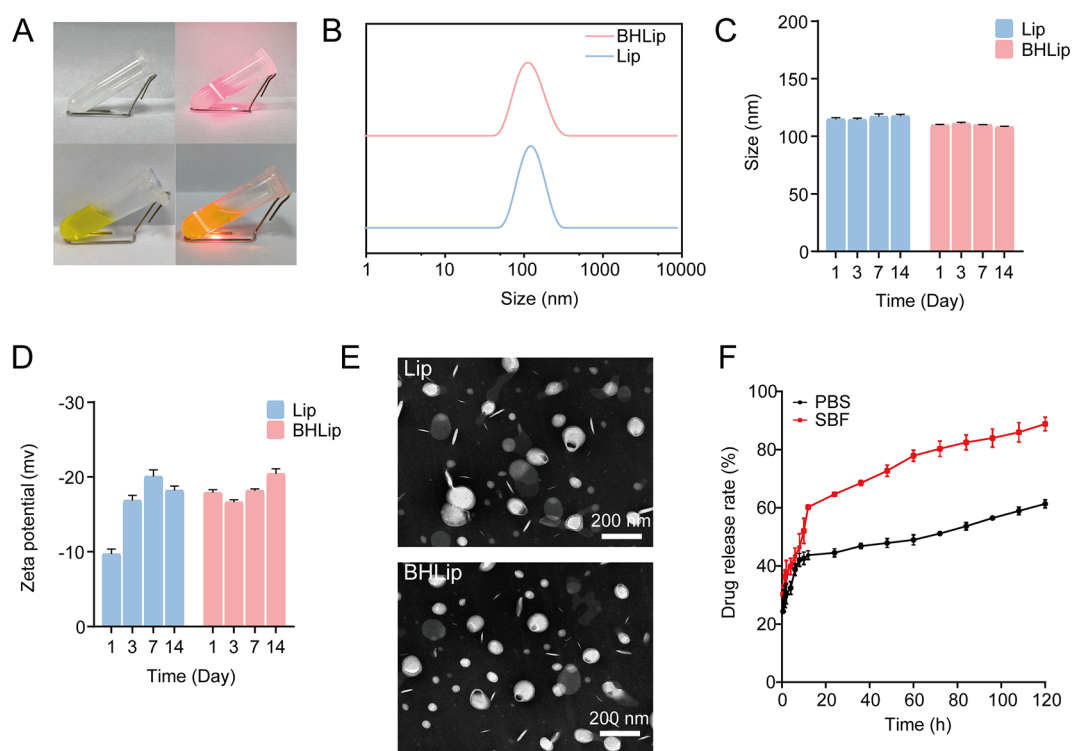
Figure 1. Preparation and characterization of liposomes and berberine liposomes. (A) Liposomes and berberine liposomes with the Tyndall effect. (B) Particle size distribution. (C) Particle size and (D) zeta potential plots within 14 days. (E) TEM image of blank liposomes and berberine-loaded liposomes. (F) Release profiles of berberine liposomes in PBS and SBF solutions (120 h) (n = 3).

and antioxidant properties.[18] It exhibits potent antibacterial activity against *S. aureus* while causing minimal side effects.[19,20] Moreover, Zhang et al. demonstrated that berberine inhibits the bacterial population-sensing Agr system, which subsequently suppresses *S. aureus* biofilm formation.[21]

Bone cements, such as poly (methyl methacrylate) (PMMA), calcium phosphate, and calcium sulfate, are utilized as fillers and drug carriers in the treatment of osteomyelitis.[22] Given the superior mechanical properties and biocompatibility of calcium sulfate bone cement, we employed a combination of berberine liposomes and calcium sulfate bone cement to treat tibial osteomyelitis in this study. We hypothesized that this berberine liposome-modified bone cement could efficiently remove biofilm from the infection site and promote bone repair. In this study, we first examined the effects of berberine-loaded liposomes on *S. aureus* and biofilm, then loaded berberine liposomes onto calcium sulfate bone cement, examined the drug release and degradation properties of berberine liposome-modified calcium sulfate bone cement, and investigated the in vitro antimicrobial properties of this bone cement. Finally, we applied berberine liposome-modified calcium sulfate bone cement in situ to the site of bone infection in rats, which effectively cleared the biofilm and promoted bone repair. This bone cement has a good prospect for clinical application in the treatment of *Staphylococcus aureus*-induced osteomyelitis.

2. RESULTS AND DISCUSSION

2.1. Successful Preparation of Berberine-Loaded Liposomes.
The main reasons why bacterial infections are difficult to cure are bacterial resistance to antibiotics and biofilm formation.[23] Liposomes can effectively penetrate the biofilm and rupture under the action of bacterial toxins,

releasing drugs into the biofilm cells and removing bacteria.[24,25] When a beam of light passes through a colloid, a bright "pathway" that appears in the colloid can be observed from the perpendicular direction of the incident light, which is the Tyndall effect.[26] The lipid bilayer structure of liposomes causes light to scatter as it passes through the liposome, producing the Tyndall phenomenon. The berberine liposomes that we prepared showed a clear Tyndall effect, indicating that a stable colloidal system of liposomes was formed (Figure 1A). The encapsulation rate of berberine liposomes was 80%, and the drug loading was 7.4%. The particle sizes of both liposomes and berberine-loaded liposomes were around 110 nm, indicating that the liposomes could encapsulate berberine well and the addition of berberine would not affect the structure and size of the liposomes (Figure 1B). Both the liposomes and berberine-loaded liposomes remained stable for 14 days (Figure 1C). The zeta potential showed that the surface of both liposomes and berberine-loaded liposomes was negatively charged (Figure 1D). The polydispersity index (PDI) was less than 0.2, and the particle size was uniform and concentrated (Figure S1A). Both liposomes and berberine-loaded liposomes were elliptical vesicles with a bilayer structure, and the outer layer seemed to be a shell wrapping the inner layer (Figure 1E). The berberine-loaded liposomes could be released continuously and slowly in both PBS and SBF solutions (Figures 1F and S1B), laying the foundation for the subsequent clearance effect of berberine liposomes on *S. aureus* and biofilm. The release of berberine-loaded liposomes in SBF solution was faster than that in PBS solution, and we hypothesized that this might be related to the composition and pH of the release medium. The pH and ionic strength of the SBF solution made it easier for berberine to dissociate from the liposomes, thus accelerating the rate of release. In addition to
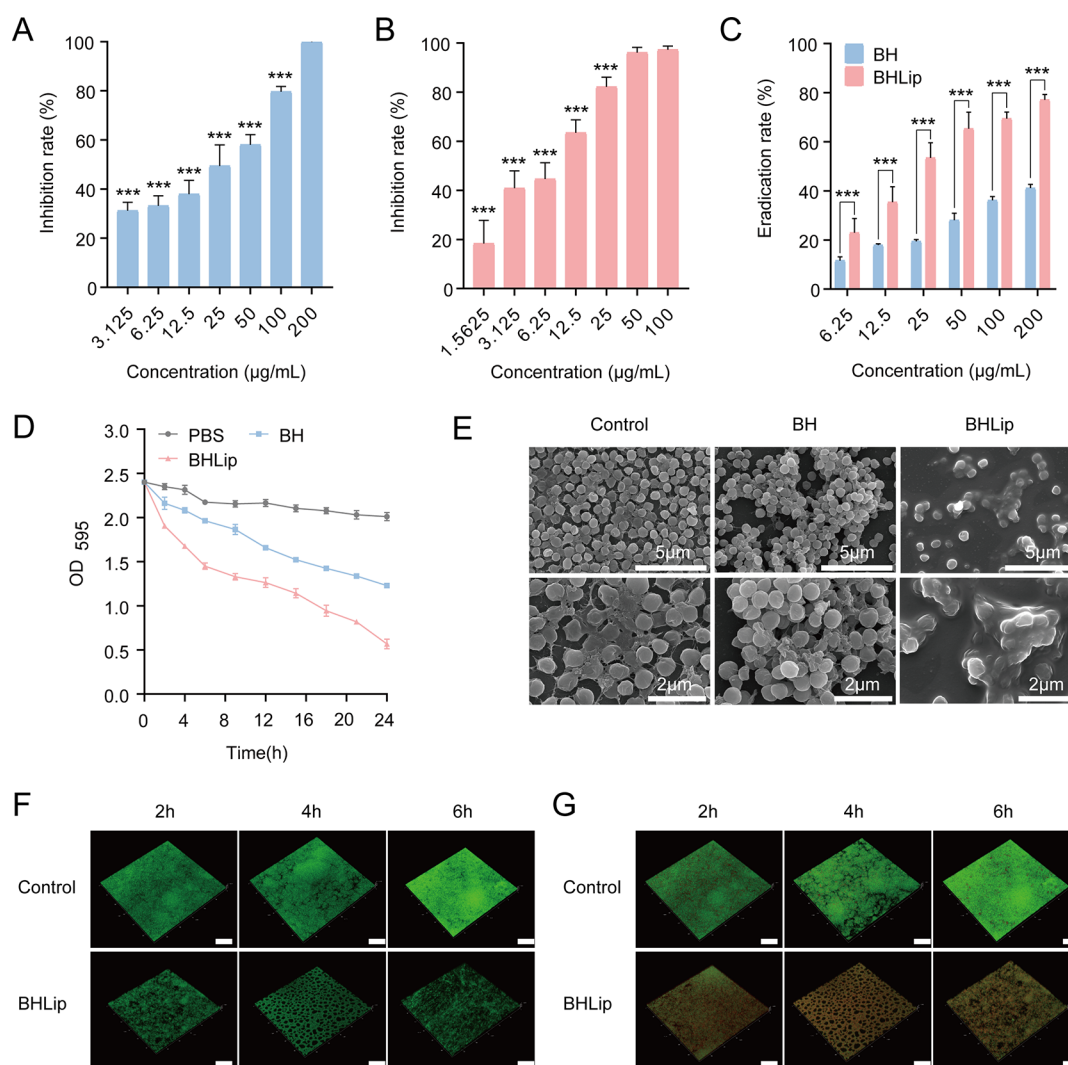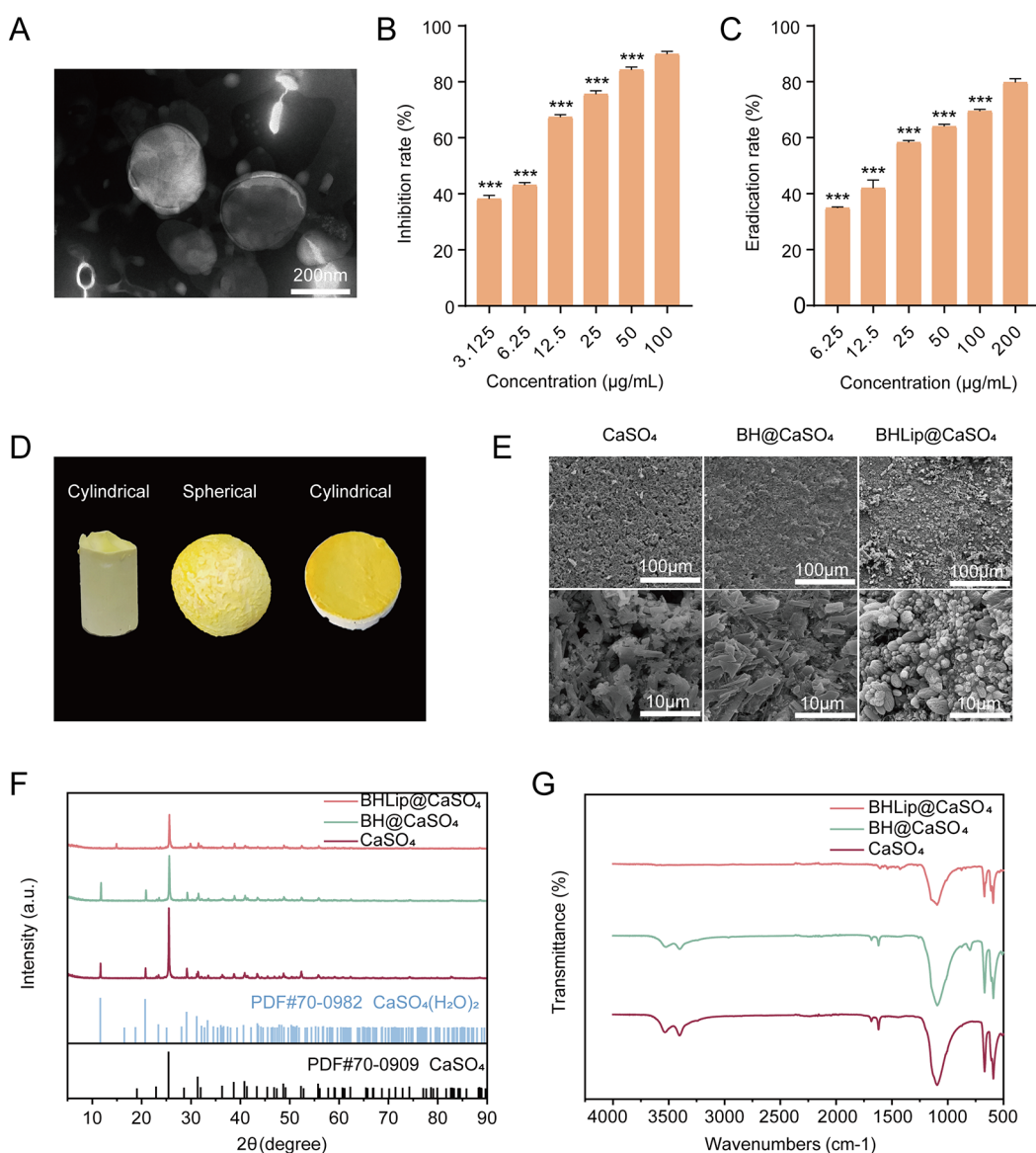
Figure 2. Eradication of *S. aureus* biofilm by berberine and berberine liposomes. (A, B) Inhibitory effect of free berberine and berberine liposome solution on *S. aureus* (n = 6/group). Showing mean ± SD, *P < 0.05, **P < 0.01, and ***P < 0.001 when compared with the highest drug concentration group. (C) Determination of biofilm eradication by the CV method (n = 6/group). Showing mean ± SD, *P < 0.05, **P < 0.01, and ***P < 0.001 when different drugs with the same concentration were compared. (D) Temporal eradication curves of biofilms (n = 6/group). (E) Scanning electron microscopy (SEM) images of biofilm. (F) Confocal microscopic images of live-stained and live−dead-stained (G) *S. aureus* biofilms, bar = 50 μm.

the buffer components such as phosphate, which were similar to those of PBS, the SBF solution also contained a variety of ions such as calcium and magnesium. These ions may interact with the membrane components of berberine liposomes, affecting liposome stability and membrane permeability. For example, calcium ions can bind to phospholipids on the liposome membrane, altering the structure and charge distribution of the membrane and increasing its permeability, thus accelerating the release of berberine.[27] In PBS solution, the ionic species and concentrations are relatively single. The pH gradient and ionic concentration difference between inside and outside the liposome membrane are small, which is not conducive to transmembrane diffusion and release of berberine. The liposome can maintain a relatively stable structure, in which the drug is released at a relatively slow rate.

2.2. Antimicrobial Properties of Berberine-Loaded Liposomes. Herein, the inhibitory effects of berberine solution and berberine-loaded liposomes on *S. aureus* were investigated using a bacterial inhibition assay. As shown in Figure 2A,B, the minimum inhibitory concentration (MIC) of

berberine solution against *S. aureus* was 100 μg/mL, and that of berberine-loaded liposomes was 50 μg/mL. When the berberine concentration was 25 μg/mL, the inhibition rate of berberine solution against *S. aureus* was only about 40%, while that of berberine-loaded liposomes was about 80%, suggesting that liposomes as a carrier greatly improved the *S. aureus* inhibition effect of berberine. Given that bacteria tend to form biofilms rather than exist as free-floating cells when infected, we then determined the eradicating effect of berberine-loaded liposomes on the *S. aureus* biofilm by the crystal violet (CV) method (Figure 2C) and XTT assay (Figure S1C). The results showed that berberine-loaded liposomes have a strong eradicating capacity on the *S. aureus* biofilm. When the berberine concentration was 50 μg/mL, the eradication rate of berberine-loaded liposomes was 75%, while that of berberine solution with the same concentration was only 40%, indicating that liposomes as carriers can be well fused with the biofilm and can release berberine to exert bacteriostatic effects.

To further demonstrate the high eradicating capacity of berberine-loaded liposomes on the *S. aureus* biofilm, we

Figure 3. Preparation and characterization of berberine liposome-modified calcium sulfate bone cement. (A) TEM images of berberine liposomes after reconstitution of spray-dried powder. (B) Inhibition and (C) eradication of the *S. aureus* biofilm by berberine liposome spray-dried powder after reconstitution ($n = 6$/group). (D) Different shapes of BHLip@CaSO$_4$: cylindrical and spherical. (E) SEM, (F) XRD, and (G) FTIR images of CaSO$_4$, BH@CaSO$_4$, and BHLip@CaSO$_4$. Showing mean ± SD, *$P < 0.05$, **$P < 0.01$, and ***$P < 0.001$ when compared with the highest drug concentration group.

determined its temporal eradication by the CV method. As shown in Figure 2D, the biofilm gradually decreased with the continuation of administration time, and the biofilm eradication of berberine-loaded liposomes was better than that of the berberine solution at all time points. Scanning electron microscopy (SEM) results showed that bacteria in the biofilm were reduced after berberine solution treatment; however, there were still a large number of *S. aureus* aggregates. In comparison, the biofilm was greatly damaged and almost invisible after treatment with berberine-loaded liposomes (Figure 2E). From the images presented by confocal microscopy (Figure 2F), it was found that berberine-loaded liposomes had a significant dispersing effect on the *S. aureus* biofilm. After treatment with berberine-loaded liposomes for 2 h, the thickness of the biofilm decreased from 24 to 16 μm, with dispersed bacteria and reduced bacterial density. Bacterial death within the biofilm could also be seen in the images

(Figure 2G), indicating that berberine liposomes entered the interior of the biofilm and released the drug to kill the bacteria.

2.3. Successful Preparation of Berberine Liposome-Modified Calcium Sulfate Bone Cement. In recent years, calcium sulfate (CaSO$_4$) has received widespread attention as an excellent bone graft material. CaSO$_4$ is almost completely absorbed in the body without causing significant inflammatory reactions, which is its most notable and excellent property as an implant material.[28,29] To facilitate storage and use, we spray-dried the liquid liposomes into a solid powder and mixed them with calcium sulfate powder to prepare berberine liposome-modified calcium sulfate bone cement (BHLip@CaSO$_4$). The lipid content of bone cement was 1%, and the berberine content was 0.1%. Transmission electron microscopy (TEM) revealed that the liposomes did not change their bilayer lipid vesicle structure after spray-drying (Figure 3A). Moreover, bacteriological experiments proved that the
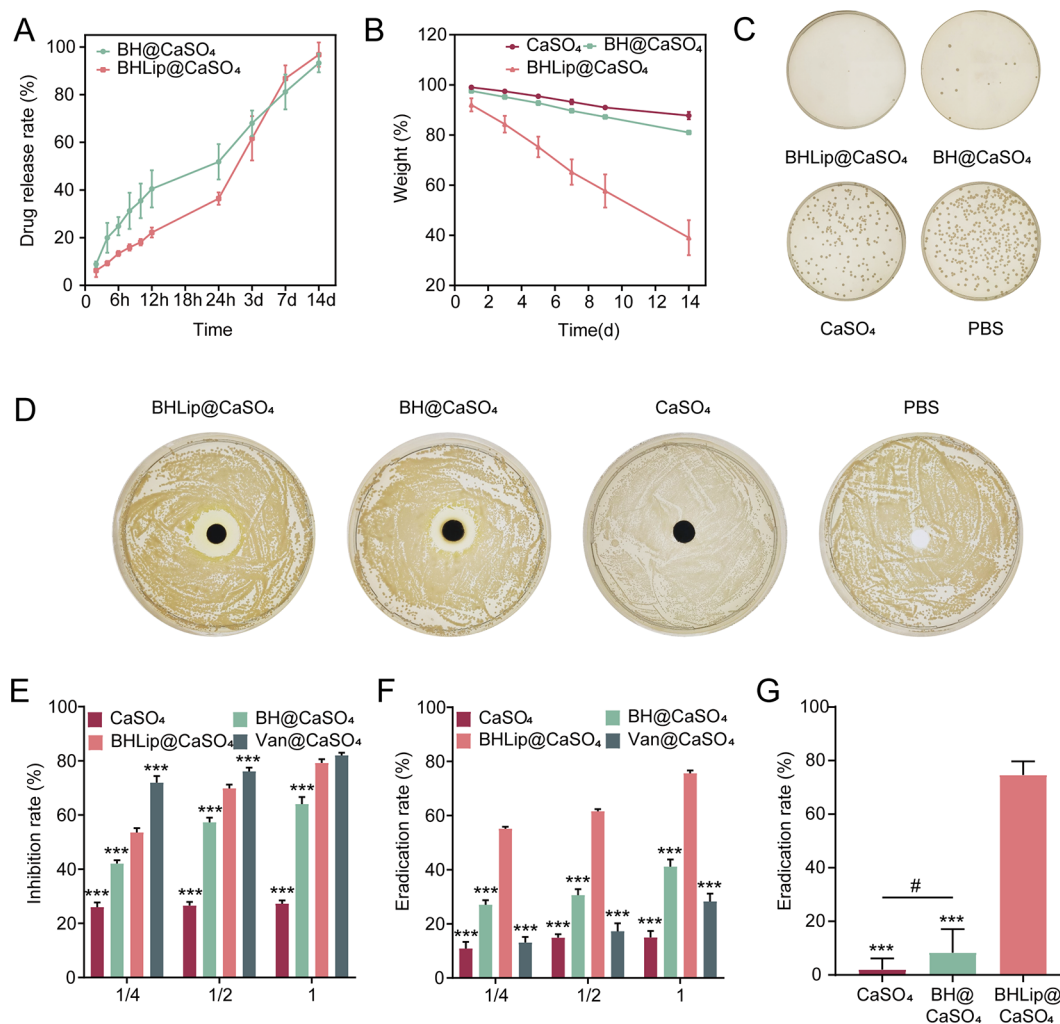
Figure 4. Inhibition of *S. aureus* by berberine liposome-modified calcium sulfate bone cement. (A) Release curve and (B) degradation curve of BHLip@CaSO$_4$ and BH@CaSO$_4$ in SBF solution ($n = 3$). (C) Colony growth after coculture of bone cement with *S. aureus*. (D) Circle of inhibition assay. (E) Inhibition and (F) eradication of *S. aureus* by CaSO$_4$, BHLip@CaSO$_4$, BH@CaSO$_4$, and Van@CaSO$_4$ extracts ($n = 6$/group). (G) Eradication of the *S. aureus* biofilm by bone cements ($n = 6$/group). Showing mean ± SD, *$P < 0.05$, **$P < 0.01$, and ***$P < 0.001$ when compared with the BHLip@CaSO$_4$ group. #$P < 0.05$, ##$P < 0.01$, and ###$P < 0.001$ when compared with the BH@CaSO$_4$ group.

redissolved berberine-loaded liposomes could effectively inhibit *S. aureus* bacteria and were able to remove *S. aureus* biofilms well (Figure 3B,C).

BHLip@CaSO$_4$ was made into cylindrical and spherical shapes through a mold (Figure 3D). SEM pictures showed a dense crystal structure on the surface of CaSO$_4$, while the surface micromorphology of berberine-modified calcium sulfate bone cement (BH@CaSO$_4$) was roughly the same as that of CaSO$_4$, indicating that the berberine-loaded liposomes were successfully embedded in calcium sulfate bone cement (Figure 3E). As shown in Figure 3F, the XRD patterns of three types of bone cement were consistent with the standard patterns of calcium sulfate dihydrate (PDF: 70-0982) or calcium sulfate (PDF: 70-0909), suggesting that the loading of berberine or berberine liposomes did not change the crystal structure of calcium sulfate bone cement material.

To further verify whether the drug was loaded into the bone cement, we performed Fourier transform infrared (FTIR) absorption spectroscopy. As shown in Figure 3G, the absorption peaks at 660 and 1087 cm^{-1} were due to the stretching and vibration of SO$_4{}^{2-}$, and the absorption peaks at 1620 and 1686 cm^{-1} were the stretching vibration peaks of OH, which indicated that the main component of bone cement was calcium sulfate hydrate. The absorption peaks at about 1260 cm^{-1} were the respiratory vibration of a benzene ring, and the absorption peaks at about 1472 cm^{-1} were the in-plane oscillation of C−H in methoxyl, which indicated that berberine was successfully loaded in both BH@CaSO$_4$ and BHLip@CaSO$_4$.

2.4. Release and Antibacterial Effects of Bone Cement.

The release test is an important index to reflect the release performance of a drug-loaded material with a long-lasting antibacterial effect. As shown in Figure 4A, both BH@CaSO$_4$ and BHLip@CaSO$_4$ showed a slow-release pattern in the first 24 h. Although the release rate of BHLip@CaSO$_4$ was accelerated after 24 h, both of them completed the release process in 14 days. The release test showed that the release rate of berberine was uniform and long-lasting, which could provide a good long-lasting antimicrobial effect.

One of the advantages of calcium sulfate as a bone repair material is that it can be degraded without the need for secondary removal. As shown in Figure 4B, CaSO$_4$ degraded slowly with a relatively uniform degradation rate throughout 14 days, reflecting the fact that this calcium sulfate material can be
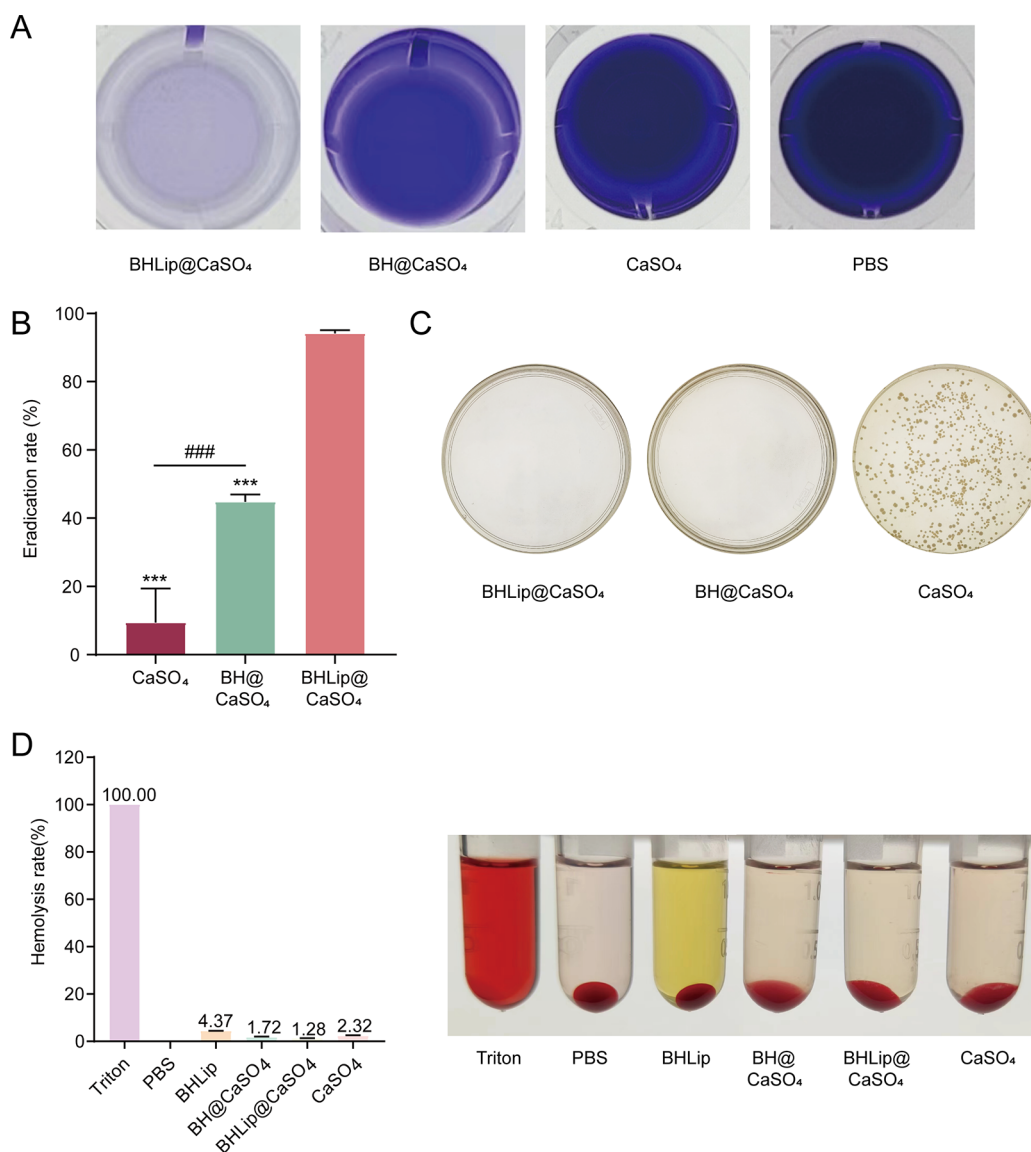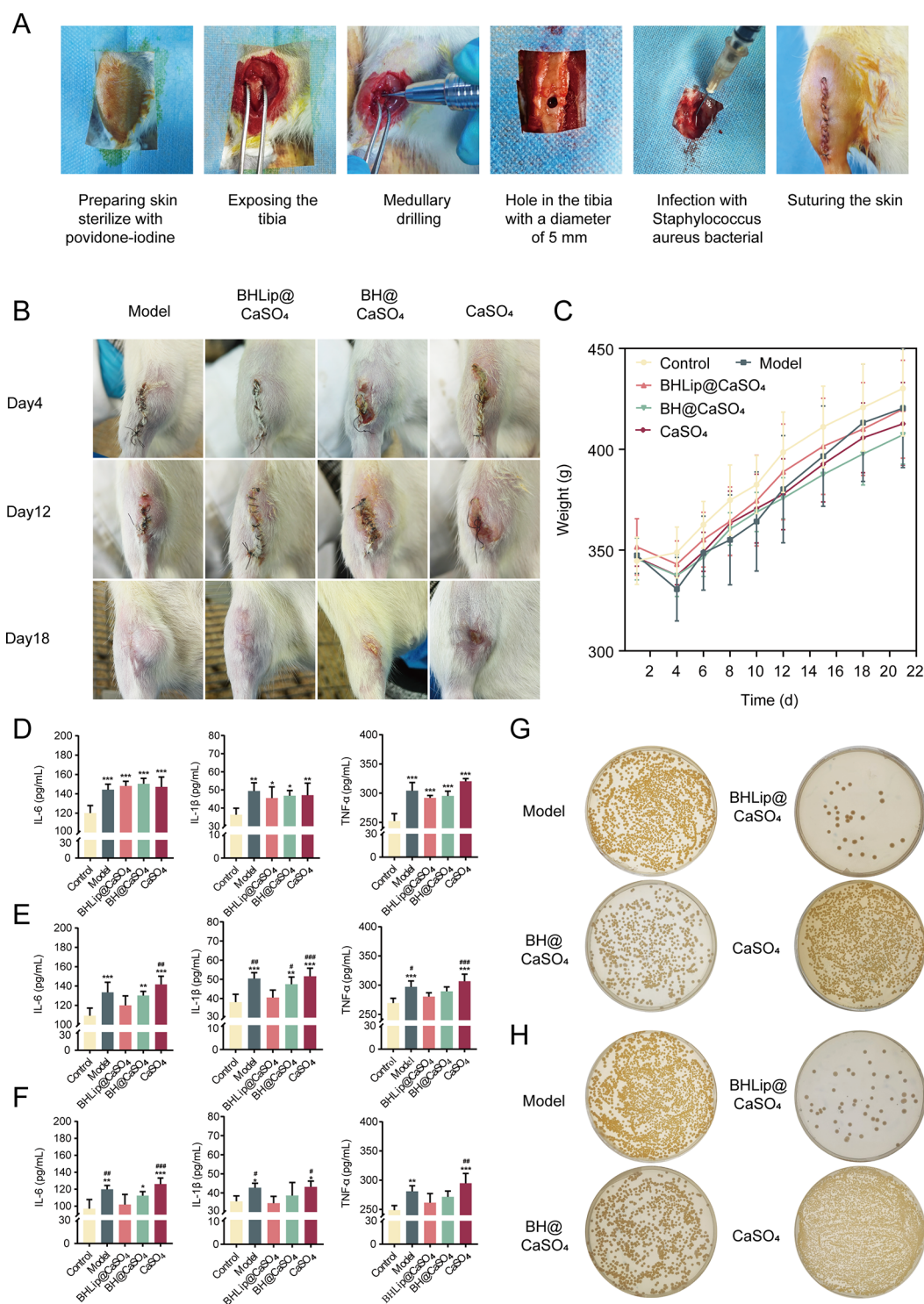
Figure 5. Effect of berberine liposome-modified calcium sulfate bone cement on biofilms. (A) Crystalline violet-stained well plates. (B) Eradication of the *S. aureus* biofilm in biofilm formation experiments ($n = 6$/group). (C) Dilution coating results of bone cement. (D) Hemolytic activity of bone cement extracts and berberine liposome solution ($n = 4$/group). Showing mean $\pm$ SD, $*P < 0.05$, $**P < 0.01$, and $***P < 0.001$ when compared with the BHLip@CaSO$_4$ group. $\#P < 0.05$, $\#\#P < 0.01$, and $\#\#\#P < 0.001$ when compared with the BH@CaSO$_4$ group.

used as a more stable drug carrier for a long time. BHLip@CaSO$_4$ degraded faster than CaSO$_4$ and BH@CaSO$_4$, probably because the loading of the liposome made the pores of the bone cement larger. There was no particular fluctuation in the degradation rate throughout the process, and the degradation was up to about 40% on the 14th day. Meanwhile, we measured the pH changes of the solution during the degradation process (Figure S1D); results showed that the pH of the bone cement soaking solution of the three groups was stabilized at around 7.8 during the whole 14 days of testing.

We applied berberine liposome-modified calcium sulfate bone cement loaded with 0.025, 0.05, and 0.1% berberine to *S. aureus* biofilms and found that the biofilm clearance was dose-dependent. When the drug loading was 0.1%, the eradication rate reached 75% (Figure S2). Therefore, we set the drug loading at 0.1%. To assess the inhibitory effect of bone cement on *S. aureus*, the colony counting method was used to evaluate

its antimicrobial performance. As shown in Figure 4C, BHLip@CaSO$_4$ had the best antibacterial performance, followed by BH@CaSO$_4$, both of which could significantly inhibit *S. aureus* bacteria, while CaSO$_4$ had almost no antibacterial effect. In addition, we used the perforation method to evaluate the antimicrobial performance again. As shown in Figure 4D, BHLip@CaSO$_4$ showed a more excellent antibacterial effect than BH@CaSO$_4$, while CaSO$_4$ had no antibacterial effect, again verifying that berberine and berberine liposome could be released from the bone cement and exert antibacterial effects. We then applied the bone cement extract to *S. aureus* and its biofilm.

As shown in Figure 4E, CaSO$_4$ had no inhibitory effect on *S. aureus*, while BHLip@CaSO$_4$ exerted an excellent antibacterial effect comparable to that of vancomycin calcium sulfate bone cement. As shown in Figure 4F, the extraction of BHLip@CaSO$_4$ had a leading eradication effect on the *S. aureus* biofilm with an eradication rate of 80%, while that of BH@CaSO$_4$ was

Figure 6. In vivo efficacy of berberine liposome-modified calcium sulfate bone cement. (A) Flowchart of rat osteomyelitis modeling. (B) Wound healing and (C) weight change of each group of rats after modeling and administration of medicine ($n = 5$/group). (D) Expression levels of inflammatory factors IL-6, IL-1β, and TNF-α in rats of each group 1 week after modeling, (E) 1 week of drug administration, and (F) after 2 weeks of drug administration ($n = 5$/group). (G) Coating results of tissue homogenate and (H) bone marrow flushing solution of bone infection site in each group. Showing mean ± SD, *$P < 0.05$, **$P < 0.01$, and ***$P < 0.001$ when compared with the control group; #$P < 0.05$, ##$P < 0.01$, and ###$P < 0.001$ when compared with the model group.

only 40%. We infer that berberine-loaded liposomes can be released from the bone cement and act on the biofilm. In contrast, vancomycin calcium sulfate bone cement, which is commonly used in clinics, cannot eradicate the biofilm, with an eradication rate of only 25%. This may be related to the resistance of the bacteria and the inability of free vancomycin to penetrate the biofilm. We then directly applied the bone cement to the *S. aureus* biofilm and found that BHLip@CaSO$_4$ still showed the strongest eradicating ability (Figure 4G).
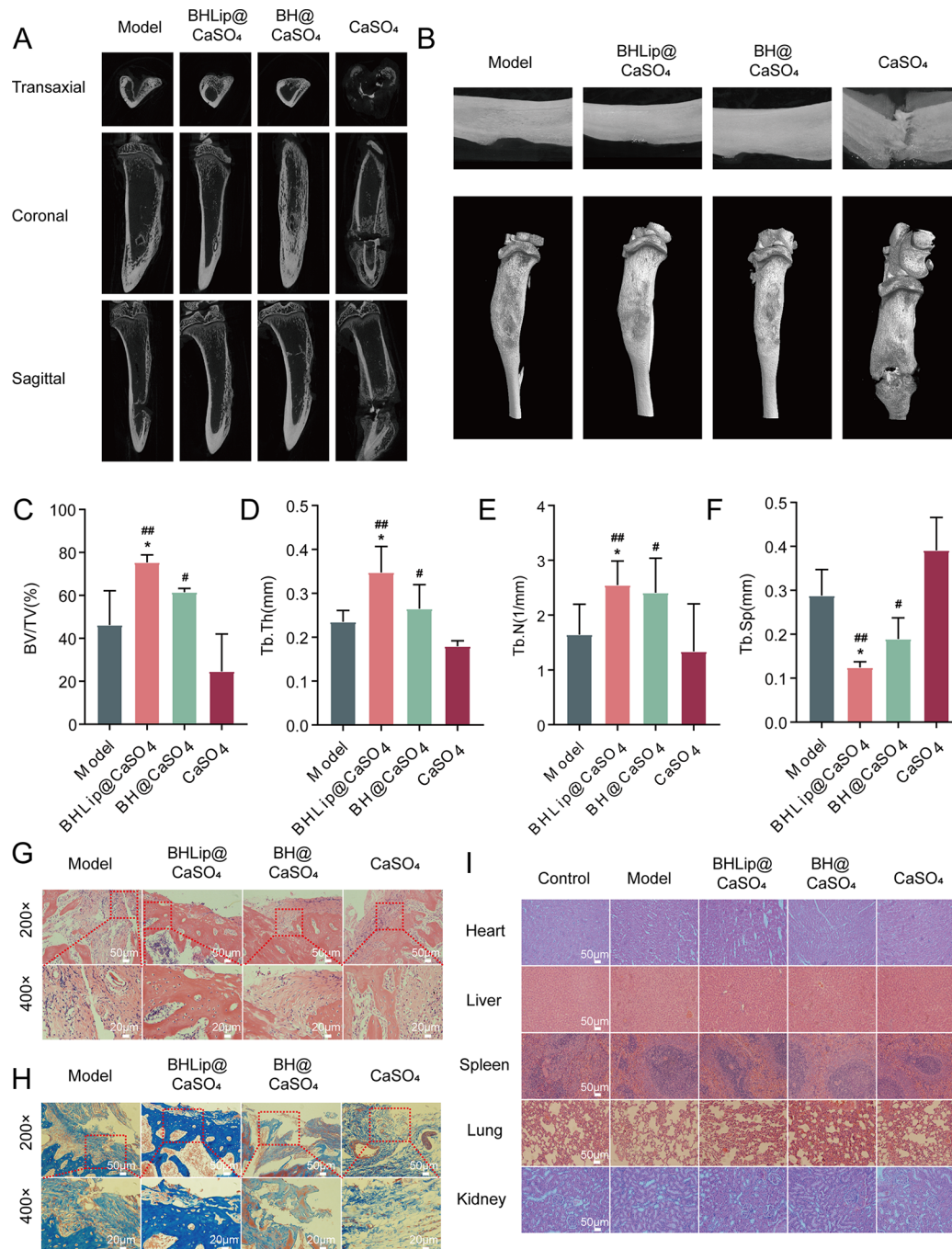
Figure 7. Micro-CT analysis and staining of pathology sections. (A) Cross-sectional, coronal, and sagittal images and (B) 3D images of the tibia (n = 3/group). (C−F) Bone parameters of rat tibia in each group (n = 3/group). (G) H&E and (H) Masson staining images of rat tibia in each group. (I) H&E staining pictures of the vital organs of rats in each group. Showing mean ± SD, *$P < 0.05$, **$P < 0.01$, and ***$P < 0.001$ when compared with the model group; #$P < 0.05$, ##$P < 0.01$, and ###$P < 0.001$ when compared with the CaSO$_4$ group.

2.5. BHLip@CaSO$_4$ Blocked the Formation of *S. aureus* Biofilm.

We examined the effect of BHLip@CaSO$_4$ on the formation of *S. aureus* biofilm and whether the biofilm would form on the surface of bone cement. As shown in Figure 5A, BHLip@CaSO$_4$ had almost no purple color, indicating that the biofilm was not formed. BH@CaSO$_4$ was not as effective as BHLip@CaSO$_4$ because *S. aureus* biofilms could still form in its presence. As shown in Figure 5B, BHLip@CaSO$_4$ prevented 95% of the biofilm formation, indicating that it had a strong antimicrobial effect and was able to prevent the formation of the *S. aureus* biofilm very well. By contrast, CaSO$_4$ bone cement was not only unable to resist bacteria but also unable to affect the formation of the biofilm. As shown in Figure 5C, the surface of CaSO$_4$ bone cement formed the biofilm, whereas the surface of BHLip@CaSO$_4$ and BH@CaSO$_4$ did not form the biofilm.

Excellent blood and cell compatibility is a prerequisite for the fabrication of biomaterials. As shown in Figure 5D, the positive control (Triton x-100) tubes were completely hemolyzed. The negative control (PBS) group was hardly hemolyzed. The bone cement extract and berberine-loaded liposome solution were about the same as those in the PBS

group and hardly hemolyzed, and the hemolysis rate was less than 5%, which indicated that the prepared bone cement had good biocompatibility.

2.6. BHLip@CaSO$_4$ Reduced *S. aureus* Infection and Promoted Osteogenesis in the Osteomyelitis Model.

We next verified the therapeutic effect of BHLip@CaSO$_4$ on a rat tibial osteomyelitis model established by drilling holes in the tibia and injecting *S. aureus* (Figure 6A). As shown in Figure 6B,C, the BHLip@CaSO$_4$ group had the best recovery performance, with improved mental diets, reduced redness and swelling, and decreased purulent secretions. Although the wound also healed in the model group, there was swelling in the wound, and the abscess was not eliminated. The worst recovery was found in the CaSO$_4$ group, as the wound was not healed, and purulent secretions were still visible.

One week after modeling, the expression levels of three inflammatory factors IL-6, IL-1β, and TNF-α in the serum of each group were elevated. Compared with those of the blank control group (control), there was a statistically significant difference (*$P < 0.05$, **$P < 0.01$, ***$P < 0.001$), indicating that the modeling of rat osteomyelitis was successful (Figure 6D). One week after drug administration, as shown in Figure 6E, the levels of three inflammatory factors were significantly downregulated in the BHLip@CaSO$_4$ group compared with the blank control group and other administered groups, with significant differences compared with the blank control group ($P < 0.001$) and model group (#$P < 0.05$, ##$P < 0.01$). After 2 weeks of drug administration, the levels of three inflammatory factors in BHLip@CaSO$_4$ group were close to those in the blank control group (Figure 6F). However, the levels of IL-6, IL-1β, and TNF-α in the model group and CaSO$_4$ group were still higher than those in other groups, and there was a significant difference between the blank control group and the BHLip@CaSO$_4$ group. BH@CaSO$_4$ also reduced the expression of inflammatory factors; however, its antimicrobial effect was not as good as that of BHLip@CaSO$_4$. We deduced that it may be because osteomyelitis is mainly a biofilm infection rather than a free bacterial infection.

Bacterial enumeration is the gold standard for the diagnosis of osteomyelitis and can also well reflect the effectiveness of treatment. Therefore, we obtained granulation tissue and bone marrow washings from the site of bone infection, and then, the plate smears were performed to test the antibacterial properties in vivo. As shown in Figure 6G,H, active *S. aureus* colonies were formed in both the model group and the CaSO$_4$ group, while only sporadic *S. aureus* colonies existed in the BHLip@CaSO$_4$ group. By counting the number of bacterial colonies, we found that BHLip@CaSO$_4$ was highly effective in antibacterial tests.

2.7. BHLip@CaSO$_4$ Promoted Bone Repair.

Infection at the local defect site greatly affects the osteogenic microenvironment and hinders the process of bone regeneration. Therefore, we performed micro-CT on the rat tibia to explore the local neoplastic bone formation. As shown in Figure 7A, the cross-sectional, coronal, and sagittal images of rat tibia in each group were analyzed. Analysis in conjunction with 3D images (Figure 7B) indicated that the best bone repair effect was observed in the BHLip@CaSO$_4$ group, with continuous and smooth bone cortex, which indicated that bone regeneration and the defects were almost healed. In the BH@CaSO$_4$ group, the bone cortex was gradually repaired; however, the healing effect was not as good as that in the BHLip@CaSO$_4$ group. Little new bone was found in the

model and CaSO$_4$ group with very low bone mass and weak bone regeneration.

To further quantify bone repair effects in bone defects, we chose the bone defect area as the target area to analyze the amount of regenerated bone using micro-CT software, and the data were analyzed by micro-CT (Figure 7C–F). The results obtained had the same trend as the images. After 2 weeks of administration, the bone volume fraction (BV/TV) was 61.48 ± 1.78% in the BH@CaSO$_4$ group and 75.31 ± 3.54% in the BHLip@CaSO$_4$ group, and both were significantly higher than those of the model group (46.18 ± 15.99%, $P < 0.05$) and CaSO$_4$ group (24.65 ± 17.36%, $P < 0.01$). In addition, for the analysis of bone trabeculae, the results had a similar trend with BV/TV; the trabecular thickness (Tb.Th) and the number of trabeculae (Tb.N) were significantly higher in the BHLip@CaSO$_4$ group than in both the model group ($P < 0.05$) and the CaSO$_4$ group ($P < 0.01$). The degree of separation of the trabeculae (Tb.Sp) in the BHLip@CaSO$_4$ group was also lower than that of the model group ($P < 0.05$) and the CaSO$_4$ group ($P < 0.01$).

After micro-CT detection, we performed histological staining of decalcified tibia samples to further evaluate the in vivo antimicrobial and bone tissue repair functions. As shown in Figure 7G, obvious intraosseous inflammation and destruction of bone were visible at the site of bone infection in the model group and the CaSO$_4$ group, with no recovery of the bone cortex, a large number of inflammatory cell infiltration around the bone tissue, irregular arrangement of osteoblasts, and fewer neoplastic bone trabeculae. Inflammatory cells at the site of bone infection were reduced in the BH@CaSO$_4$ group, but nonhealing at the site of bone infection could also be observed. In the BHLip@CaSO$_4$ group, the bone infection site was healed and filled with new bone. Regular osteoblasts and gradually recovered bone cortex could be seen in the BHLip@CaSO$_4$ group, with significantly reduced inflammatory cells and dense, regular, and complete new bone. Masson staining (Figure 7H) showed that new bone tissue and collagen were significantly more abundant in the BHLip@CaSO$_4$ group than in the other groups. BHLip@CaSO$_4$ exerted superior antimicrobial and osteogenic properties.

The safety of the implanted material is a key factor for its clinical application. As shown in Figure 7I, all organs in each group of rats showed normal tissue morphology, which proved that the composite system had good bio-/histocompatibility and material systemic safety. However, this study focuses on short-term observation of therapeutic effects, such as changes in inflammatory indexes and bone healing. Researchers can extend the time of osteomyelitis modeling and treatment recovery and pay attention to the long-term prognosis of infected animals.

3. CONCLUSIONS

Osteomyelitis and bone defects caused by bacteria have increasingly become common medical problems affecting the quality of life. Currently, the design of antibiotic-loaded biodegradable biomaterials for slow-release systems has become a hot research topic in recent years. The primary mechanism of osteomyelitis pathogenesis is the formation of the *S. aureus* biofilm, which limits the efficacy of antibiotics and poses a significant challenge to bone infections. In this study, berberine-loaded liposomes were developed. The berberine-loaded liposomes not only inhibited free-floating *S. aureus*

bacteria but also eradicated the biofilm. It is expected to be utilized in osteomyelitis disease and exert antimicrobial effects; hence, we combined a berberine-loaded liposome with calcium sulfate bone cement, which is commonly used in clinical practice. In vitro experiments demonstrated that berberine-loaded liposome-modified calcium sulfate bone cement exhibited ideal drug release kinetics and degradability. Moreover, its biofilm-eradicating capacity was much higher than that of the clinically used vancomycin calcium sulfate bone cement. In vivo experiments have shown that BHLip@CaSO₄ is effective in treating osteomyelitis. BHLip@CaSO₄ could also promote osteogenesis, which was related to its excellent antibacterial ability. BHLip@CaSO₄ was able to be utilized as a carrier to act directly on the bone infection site and release the berberine liposome to fight against the *S. aureus* biofilm, thus exerting excellent antimicrobial effects. However, the present study focused on the antimicrobial ability of BHLip@CaSO₄, and the mechanism study of its osteogenic effect is still shallow. We will continue to research the antimicrobial and osteogenic mechanisms of BHLip@CaSO₄ in the future.

4. MATERIALS AND METHODS

4.1. Materials. Berberine was purchased from Liangwei Biotechnology Co., Ltd. (Nanjing, China). Hydrogenated soy lecithin (HSPC), cholesterol (Chol), and distearoylphosphatidylethanolamine-polyethylene glycol 2000 (DSPE-MPEG2000) were purchased from A. V. T. Pharmaceutical Technology Co. (Shanghai, China). *Staphylococcus aureus* (ATCC25923) was purchased from Solarbio Science Technology Co., Ltd. (Beijing, China). ELISA kits were purchased from Nanjing Yifeixue Biotechnology Co., Ltd. (Nanjing, China). All other reagents were commercially purchased and were not further purified.

4.2. Preparation, Characterization, and Release of Berberine Liposomes. The liposome preparation protocol was slightly modified from previous studies.[30] We prepared blank liposomes by the film dispersion method. HSPC, Chol, and DSPE-MPEG2000 with a molar ratio of 45:50:5 were dissolved with anhydrous ethanol and placed in a cigar-shaped flask to form a lipid film. Later, a citrate buffer solution was added to form a lipid suspension. Then, the lipid suspension was extruded through a polycarbonate membrane with a pore size of 0.1 μm 11 times, yielding a liposome solution with uniform particle size. Berberine liposomes were prepared by the pH gradient method. The liposome solution was mixed with 1 mg/mL berberine solution, and 0.595 mM NaHCO₃ solution was slowly added to adjust the pH of the solution to neutrality. The particle size and zeta potential were determined by dynamic light scattering. The morphology and structure of liposomes were characterized by TEM. The drug release experiment was carried out by the dialysis bag method.[31,32] With PBS and SBF as dissolution media, berberine liposomes were placed in 8000−14,000 Da dialysis bags and placed in a 37 °C shaker at 100 rpm to determine the drug release rate. Each sample was prepared in triplicate. The drug concentration was determined by HPLC. The determination was performed on a Hedera ODS-2 (4.6 × 250 mm) column at 30 °C, a detection wavelength at 345 nm, and a mobile phase consisting of acetonitrile (C): 0.05% ethylenediamine − 0.1% phosphoric acid water (D) = 35:65. The flow rate of the mobile phase was 0.8 mL/min.

4.3. Antimicrobial Assay of Berberine Liposomes. The concentration of *S. aureus* added in the experiment was 10⁶ CFU/mL. The MIC assay was determined by the micro broth dilution method (enzyme-labeled plate) according to the standard method of CLSI.[33,34] The lowest concentration of the drug at which there was no growth of bacteria on the 96-well plates with the naked eye after 24 h was taken as the MIC value. The OD$_{600}$ was measured using an enzyme labeling instrument to calculate the inhibition rate. Subsequently, we applied berberine liposomes to the biofilm, which was quantitatively determined by the crystalline violet (CV) method[35] or the XTT method.[36] The OD$_{595}$ was measured to calculate the eradication rate. Berberine liposomes were applied to cell crawls with the biofilm, and the structure of the biofilm was observed by SEM and CLSM.

4.4. Preparation and Characterization of Bone Cement. Berberine liposome solution was spray-dried with a spray dryer. Then, berberine liposome powder was mixed with calcium sulfate powder to make a berberine liposome-modified calcium sulfate bone cement. Making the berberine content of 0.1%, ultrapure water was the hydration solution, and the solid−liquid ratio was 0.6 mL/g. The bone cement was ground into powder for XRD detection[37] and FTIR assay.[38] Later, we immersed the bone cement in 8 mL of SBF solution and put it in a 37 °C shaker at 100 rpm to calculate the cumulative release rate. The bone cement was immersed in 5 mL of SBF solution in a 37 °C shaker at 100 rpm. Bone cement was removed at a fixed point to dry and weigh, and the degradation rate was calculated.

4.5. Antimicrobial Assay of Berberine Liposome-Modified Calcium Sulfate Bone Cement. Bone cements were cocultured with *S. aureus*, and the bacterial solution was spread on TSA solid agar plates to observe the growth of the colonies. *S. aureus* bacterial solution was evenly coated on the TSA agar plate, and then, holes with a diameter of 10 mm in the TSA agar plate were punched, and cylindrical bone cement was placed in the holes. The TSA agar plate was incubated at 37 °C for 18−24 h to observe the inhibition circle.[39] The bone cement was immersed in PBS solution and removed after 24 h to obtain the bone cement extraction solution.

4.6. Animal Studies. Male SD rats were fixed in the supine position on the rat board; the right lower limb was sterilized with sterile sheets. A 1 cm long incision was made in the proximal anterior metaphysis of the tibia; the skin, subcutaneous tissue, and fascia were incised to separate the muscles and expose the tibia. The bone marrow of the middle tibia was aspirated by using a 1.0 mm dental drill to penetrate the cortical drill hole. 100 μL of bacterial solution (1×10^8 CFU/mL) was injected into the bone marrow cavity, the hole was sealed with bone wax to prevent bacterial leakage, the fascia and skin were sutured, and the incision was sterilized with iodine povidone and carefully bandaged.[40] One week after molding, the infected area was debrided, molded bone cement was implanted to completely fill the drilled area, and the skin was sutured. We measured the levels of the inflammatory factors at different stages. Tissue homogenate and bone marrow rinse were coated on TSA to compare the antimicrobial capacities of bone cements. The rat tibia samples were scanned using micro-CT, and the bone parameters were analyzed by CTAn.

The animal protocols were approved and conducted by the Guide for the Care and Use of the Laboratory Animal Center at Nanjing University of Chinese Medicine. All procedures

were in accordance with the Guide for the Care and Use of Laboratory Animals (National Institutes of Health).

Detailed experimental methods are described in the Supporting Information.

4.7. Statistical Analysis. All the data in this study were statistically analyzed by one-way ANOVA (intergroup comparisons) and Student's *t*-test (intragroup comparisons). The values were presented as mean $\pm$ standard deviation (SD), and $P < 0.05$ was considered statistically significant (*$P < 0.05$, **P, ***$P < 0.01$).

■ ASSOCIATED CONTENT

Data Availability Statement

Data will be made available on request.

⑤ Supporting Information

The Supporting Information is available free of charge at https://pubs.acs.org/doi/10.1021/acsomega.4c11198.

> Detailed methods of the experiment; polymer dispersity index (PDI) of blank liposomes and berberine liposomes within 14 days, release profiles of berberine liposome in PBS and SBF solutions (24 h), eradication rate of berberine liposome as determined by XTT methods, and pH change curve of bone cement; and eradication rate of bone cement with drug loadings of 0.025, 0.05, and 0.1% (PDF)

■ AUTHOR INFORMATION

Corresponding Authors

Shaoguang Li − *Microsurgery Department of Senior Department of Orthopedics, The Fourth Medical Center of PLA General Hospital, Beijing 100048, China*; Email: drshaoguang@163.com

Tingming Fu − *State Key Laboratory on Technologies for Chinese Medicine Pharmaceutical Process Control and Intelligent Manufacture, Nanjing University of Chinese Medicine, Nanjing 210023, China*; ⓞ orcid.org/0000-0003-4196-6787; Email: futm@njucm.edu.cn

Authors

Siting Wang − *State Key Laboratory on Technologies for Chinese Medicine Pharmaceutical Process Control and Intelligent Manufacture, Nanjing University of Chinese Medicine, Nanjing 210023, China*

Tianlong Zhao − *State Key Laboratory on Technologies for Chinese Medicine Pharmaceutical Process Control and Intelligent Manufacture, Nanjing University of Chinese Medicine, Nanjing 210023, China*

Yuping Sun − *State Key Laboratory on Technologies for Chinese Medicine Pharmaceutical Process Control and Intelligent Manufacture, Nanjing University of Chinese Medicine, Nanjing 210023, China*

Sipan Li − *State Key Laboratory on Technologies for Chinese Medicine Pharmaceutical Process Control and Intelligent Manufacture, Nanjing University of Chinese Medicine, Nanjing 210023, China*

Danya Lu − *State Key Laboratory on Technologies for Chinese Medicine Pharmaceutical Process Control and Intelligent Manufacture, Nanjing University of Chinese Medicine, Nanjing 210023, China*

Mengmeng Qiu − *State Key Laboratory on Technologies for Chinese Medicine Pharmaceutical Process Control and Intelligent Manufacture, Nanjing University of Chinese Medicine, Nanjing 210023, China*

Baofei Yan − *State Key Laboratory on Technologies for Chinese Medicine Pharmaceutical Process Control and Intelligent Manufacture, Nanjing University of Chinese Medicine, Nanjing 210023, China*; ⓞ orcid.org/0000-0002-6754-7655

Jingwen Yang − *State Key Laboratory on Technologies for Chinese Medicine Pharmaceutical Process Control and Intelligent Manufacture, Nanjing University of Chinese Medicine, Nanjing 210023, China*

Zhitao Shao − *State Key Laboratory on Technologies for Chinese Medicine Pharmaceutical Process Control and Intelligent Manufacture, Nanjing University of Chinese Medicine, Nanjing 210023, China*

Yuqi Yin − *State Key Laboratory on Technologies for Chinese Medicine Pharmaceutical Process Control and Intelligent Manufacture, Nanjing University of Chinese Medicine, Nanjing 210023, China*

Complete contact information is available at:
https://pubs.acs.org/10.1021/acsomega.4c11198

Author Contributions

S.W.: Writing—review and editing, writing—original draft, validation, methodology, investigation, formal analysis, and data curation. T.Z.: Writing—review and editing and formal analysis. Y.S.: Investigation. S.L.: Methodology and formal analysis. D.L.: Investigation. M.Q.: Methodology. B.Y.: Supervision. J.Y.: Validation. Z.S.: Investigation. Y.Y.: Investigation. S.L.: Supervision and project administration. T.F.: Writing—review and editing, supervision, project administration, formal analysis, and conceptualization. S.W. and T.Z. contributed equally.

Notes

The authors declare no competing financial interest.

■ ACKNOWLEDGMENTS

■ REFERENCES

(1) Ak, G.; Bozkaya Ü, F.; Yılmaz, H.; Sarı Turgut, Ö.; Bilgin, İ.; Tomruk, C.; Uyanıkgil, Y.; Hamarat Şanlıer, Ş. An intravenous application of magnetic nanoparticles for osteomyelitis treatment: An efficient alternative. *Int. J. Pharm.* **2021**, *592*, No. 119999.

(2) Dudareva, M.; Hotchen, A. J.; Ferguson, J.; Hodgson, S.; Scarborough, M.; Atkins, B. L.; McNally, M. A. The microbiology of chronic osteomyelitis: Changes over ten years. *J. Infect* **2019**, *79* (3), 189−198.

(3) Kavanagh, N.; Ryan, E. J.; Widaa, A.; Sexton, G.; Fennell, J.; O'Rourke, S.; Cahill, K. C.; Kearney, C. J.; O'Brien, F. J.; Kerrigan, S. W. Staphylococcal Osteomyelitis: Disease Progression, Treatment Challenges, and Future Directions. *Clin. Microbiol. Rev.* **2018**, *31* (2), No. e00084-17.

(4) Lew, D. P.; Waldvogel, F. A. Osteomyelitis. *Lancet* **2004**, *364* (9431), 369−379.

(5) Ricciardi, B. F.; Muthukrishnan, G.; Masters, E.; Ninomiya, M.; Lee, C. C.; Schwarz, E. M. Staphylococcus aureus Evasion of Host Immunity in the Setting of Prosthetic Joint Infection: Biofilm and Beyond. *Curr. Rev. Musculoskelet Med.* **2018**, *11* (3), 389−400.

(6) Masters, E. A.; Trombetta, R. P.; de Mesy Bentley, K. L.; Boyce, B. F.; Gill, A. L.; Gill, S. R.; Nishitani, K.; Ishikawa, M.; Morita, Y.; Ito, H.; et al. Evolving concepts in bone infection: redefining "biofilm", "acute vs. chronic osteomyelitis", "the immune proteome" and "local antibiotic therapy". *Bone Res.* 2019, 7, 20.

(7) Hall, C. W.; Mah, T. F. Molecular mechanisms of biofilm-based antibiotic resistance and tolerance in pathogenic bacteria. *FEMS Microbiol Rev.* 2017, 41 (3), 276−301.

(8) Nandi, S. K.; Bandyopadhyay, S.; Das, P.; Samanta, I.; Mukherjee, P.; Roy, S.; Kundu, B. Understanding osteomyelitis and its treatment through local drug delivery system. *Biotechnol Adv.* 2016, 34 (8), 1305−1317.

(9) Bose, S.; Tarafder, S. Calcium phosphate ceramic systems in growth factor and drug delivery for bone tissue engineering: a review. *Acta Biomater* 2012, 8 (4), 1401−1421.

(10) Ghosh, S.; Sinha, M.; Samanta, R.; Sadhasivam, S.; Bhattacharyya, A.; Nandy, A.; Saini, S.; Tandon, N.; Singh, H.; Gupta, S.; et al. A potent antibiotic-loaded bone-cement implant against staphylococcal bone infections. *Nat. Biomed Eng.* 2022, 6 (10), 1180−1195.

(11) Masters, E. A.; Ricciardi, B. F.; Bentley, K. L. M.; Moriarty, T. F.; Schwarz, E. M.; Muthukrishnan, G. Skeletal infections: microbial pathogenesis, immunity and clinical management. *Nat. Rev. Microbiol* 2022, 20 (7), 385−400.

(12) Koo, H.; Allan, R. N.; Howlin, R. P.; Stoodley, P.; Hall-Stoodley, L. Targeting microbial biofilms: current and prospective therapeutic strategies. *Nat. Rev. Microbiol* 2017, 15 (12), 740−755.

(13) Rukavina, Z.; Vanić, Ž. Current Trends in Development of Liposomes for Targeting Bacterial Biofilms. *Pharmaceutics* 2016, 8 (2), 18.

(14) Forier, K.; Raemdonck, K.; De Smedt, S. C.; Demeester, J.; Coenye, T.; Braeckmans, K. Lipid and polymer nanoparticles for drug delivery to bacterial biofilms. *J. Controlled Release* 2014, 190, 607−623.

(15) Pornpattananangkul, D.; Zhang, L.; Olson, S.; Aryal, S.; Obonyo, M.; Vecchio, K.; Huang, C. M.; Zhang, L. Bacterial toxin-triggered drug release from gold nanoparticle-stabilized liposomes for the treatment of bacterial infection. *J. Am. Chem. Soc.* 2011, 133 (11), 4132−4139.

(16) Xie, J.; Meng, Z.; Han, X.; Li, S.; Ma, X.; Chen, X.; Liang, Y.; Deng, X.; Xia, K.; Zhang, Y.; et al. Cholesterol Microdomain Enhances the Biofilm Eradication of Antibiotic Liposomes. *Adv. Healthc. Mater.* 2022, 11 (8), No. e2101745.

(17) Tong, J.; Hou, X.; Cui, D.; Chen, W.; Yao, H.; Xiong, B.; Cai, L.; Zhang, H.; Jiang, L. A berberine hydrochloride-carboxymethyl chitosan hydrogel protects against Staphylococcus aureus infection in a rat mastitis model. *Carbohydr. Polym.* 2022, 278, No. 118910.

(18) Imenshahidi, M.; Hosseinzadeh, H. Berberine and barberry (Berberis vulgaris): A clinical review. *Phytother Res.* 2019, 33 (3), 504−523.

(19) Guo, N.; Zhao, X.; Li, W.; Shi, C.; Meng, R.; Liu, Z.; Yu, L. The synergy of berberine chloride and totarol against Staphylococcus aureus grown in planktonic and biofilm cultures. *J. Med. Microbiol* 2015, 64 (8), 891−900.

(20) Wojtyczka, R. D.; Dziedzic, A.; Kępa, M.; Kubina, R.; Kabała-Dzik, A.; Mularz, T.; Idzik, D. Berberine enhances the antibacterial activity of selected antibiotics against coagulase-negative Staphylococcus strains in vitro. *Molecules* 2014, 19 (5), 6583−6596.

(21) Zhang, C.; Li, Z.; Pan, Q.; Fan, L.; Pan, T.; Zhu, F.; Pan, Q.; Shan, L.; Zhao, L. Berberine at sub-inhibitory concentration inhibits biofilm dispersal in Staphylococcus aureus. *Microbiology* 2022, 168 (9), No. 001243.

(22) Ford, C. A.; Cassat, J. E. Advances in the local and targeted delivery of anti-infective agents for management of osteomyelitis. *Expert Rev. Anti Infect Ther* 2017, 15 (9), 851−860.

(23) Flemming, H. C.; Wingender, J.; Szewzyk, U.; Steinberg, P.; Rice, S. A.; Kjelleberg, S. Biofilms: an emergent form of bacterial life. *Nat. Rev. Microbiol* 2016, 14 (9), 563−575.

(24) Shah, S.; Dhawan, V.; Holm, R.; Nagarsenker, M. S.; Perrie, Y. Liposomes: Advancements and innovation in the manufacturing process. *Adv. Drug Deliv. Rev.* 2020, 154−155, 102−122.

(25) Kluzek, M.; Oppenheimer-Shaanan, Y.; Dadosh, T.; Morandi, M. I.; Avinoam, O.; Raanan, C.; Goldsmith, M.; Goldberg, R.; Klein, J. Designer Liposomic Nanocarriers Are Effective Biofilm Eradicators. *ACS Nano* 2022, 16 (10), 15792−15804.

(26) Xiao, W.; Deng, Z.; Huang, J.; Huang, Z.; Zhuang, M.; Yuan, Y.; Nie, J.; Zhang, Y. Highly Sensitive Colorimetric Detection of a Variety of Analytes via the Tyndall Effect. *Anal. Chem.* 2019, 91 (23), 15114−15122.

(27) Qing, S.; Lyu, C.; Zhu, L.; Pan, C.; Wang, S.; Li, F.; Wang, J.; Yue, H.; Gao, X.; Jia, R.; et al. Biomineralized Bacterial Outer Membrane Vesicles Potentiate Safe and Efficient Tumor Micro-environment Reprogramming for Anticancer Therapy. *Adv. Mater.* 2020, 32 (47), No. e2002085.

(28) Ene, R.; Nica, M.; Ene, D.; Cursaru, A.; Cirstoiu, C. Review of calcium-sulphate-based ceramics and synthetic bone substitutes used for antibiotic delivery in PJI and osteomyelitis treatment. *EFORT Open Rev.* 2021, 6 (5), 297−304.

(29) No, Y. J.; Roohani-Esfahani, S. I.; Zreiqat, H. Nanomaterials: the next step in injectable bone cements. *Nanomedicine (Lond)* 2014, 9 (11), 1745−1764.

(30) Li, S.; Wang, Y.; Wang, S.; Xie, J.; Fu, T.; Li, S. In situ gelling hydrogel loaded with berberine liposome for the treatment of biofilm-infected wounds. *Front. Bioeng. Biotechnol.* 2023, 11, No. 1189010.

(31) Pattni, B. S.; Chupin, V. V.; Torchilin, V. P. New Developments in Liposomal Drug Delivery. *Chem. Rev.* 2015, 115 (19), 10938−10966.

(32) Guimarães, D.; Cavaco-Paulo, A.; Nogueira, E. Design of liposomes as drug delivery system for therapeutic applications. *Int. J. Pharm.* 2021, 601, No. 120571.

(33) Nicolosi, D.; Cupri, S.; Genovese, C.; Tempera, G.; Mattina, R.; Pignatello, R. Nanotechnology approaches for antibacterial drug delivery: Preparation and microbiological evaluation of fusogenic liposomes carrying fusidic acid. *Int. J. Antimicrob. Agents* 2015, 45 (6), 622−626.

(34) Bandara, H. M.; Herpin, M. J.; Kolacny, D., Jr.; Harb, A.; Romanovicz, D.; Smyth, H. D. Incorporation of Farnesol Significantly Increases the Efficacy of Liposomal Ciprofloxacin against Pseudomonas aeruginosa Biofilms in Vitro. *Mol. Pharmaceutics* 2016, 13 (8), 2760−2770.

(35) Xu, Z.; Liang, Y.; Lin, S.; Chen, D.; Li, B.; Li, L.; Deng, Y. Crystal Violet and XTT Assays on Staphylococcus aureus Biofilm Quantification. *Curr. Microbiol.* 2016, 73 (4), 474−482.

(36) Mishra, P.; Gupta, P.; Pruthi, V. Cinnamaldehyde incorporated gellan/PVA electrospun nanofibers for eradicating Candida biofilm. *Mater. Sci. Eng. C Mater. Biol. Appl.* 2021, 119, No. 111450.

(37) Avramenko, M.; Nakashima, K.; Takano, C.; Kawasaki, S. Eco-friendly soil stabilization method using fish bone as cement material. *Sci. Total Environ.* 2023, 900, No. 165823.

(38) Ooms, E. M.; Wolke, J. G.; van de Heuvel, M. T.; Jeschke, B.; Jansen, J. A. Histological evaluation of the bone response to calcium phosphate cement implanted in cortical bone. *Biomaterials* 2003, 24 (6), 989−1000.

(39) Sun, X.; Liang, H.; Wang, H.; Meng, N.; Jin, S.; Zhou, N. Silk fibroin/polyvinyl alcohol composite film loaded with antibacterial AgNP/polydopamine-modified montmorillonite; characterization and antibacterial properties. *Int. J. Biol. Macromol.* 2023, 251, No. 126368.

(40) Tian, L.; Tan, Z.; Yang, Y.; Liu, S.; Yang, Q.; Tu, Y.; Chen, J.; Guan, H.; Fan, L.; Yu, B.; et al. In situ sprayed hydrogels containing resiquimod-loaded liposomes reduce chronic osteomyelitis recurrence by intracellular bacteria clearance. *Acta Biomater* 2023, 169, 209−227.